

Infrared reflectivity of single-crystal  
 $\text{Bi}_{2M_{m+1}\text{Co}_m\text{O}_y}$  ( $M=\text{Ca}, \text{Sr}, \text{Ba}; m=1, 2$ ),  
 $\text{Bi}_2\text{Sr}_3\text{Fe}_{20}9.2$ , and  $\text{Bi}_2\text{Sr}_2\text{MnO}_6.25$ ,  
isomorphic to Bi-Cu-based high- $T_c$  oxides

Watanabe, Yukio

Department of Electrical Engineering, Princeton University, Princeton

Tsui, D. C.

Department of Electrical Engineering, Princeton University, Princeton

Birmingham, J. T.

Department of Physics, Princeton University, Princeton

Ong, N. P.

Department of Physics, Princeton University, Princeton

他

<https://hdl.handle.net/2324/4493209>

---

出版情報 : Physical Review B. 43 (4), pp.3026-3033, 1991-02-01. American Physical Society

バージョン :

権利関係 : © 1991 The American Physical Society

**Infrared reflectivity of single-crystal  $\text{Bi}_2M_{m+1}\text{Co}_m\text{O}_y$   
( $M = \text{Ca, Sr, Ba}$ ;  $m = 1, 2$ ),  $\text{Bi}_2\text{Sr}_3\text{Fe}_2\text{O}_{9.2}$ , and  
 $\text{Bi}_2\text{Sr}_2\text{MnO}_{6.25}$ , isomorphic to Bi-Cu-based high- $T_c$  oxides**

Yukio Watanabe\* and D. C. Tsui

*Department of Electrical Engineering, Princeton University, Princeton, New Jersey 08544*

J. T. Birmingham and N. P. Ong

*Department of Physics, Princeton University, Princeton, New Jersey 08544*

J. M. Tarascon

*Bell Communications Research, Red Bank, New Jersey 07701*

(Received 19 June 1990; revised manuscript received 10 September 1990)

The infrared reflectivity of single crystals of  $\text{Bi}_2M_{m+1}\text{Co}_m\text{O}_y$  ( $M = \text{Ca, Sr, Ba}$ ;  $m = 1, 2$ ),  $\text{Bi}_2\text{Sr}_3\text{Fe}_2\text{O}_{9.2}$ , and  $\text{Bi}_2\text{Sr}_2\text{MnO}_{6.25}$  was measured at room temperature between 0.08 and 1.4 eV. A broad absorption band is observed in the mid-ir range (near 0.5 eV) in all the compounds studied, and an absorption band near 0.3 eV is observed in the insulating system. In terms of a conventional Drude-Lorentz model, the measured reflectivity and the frequency-dependent conductivity between 0.2 and 1 eV can be fitted with three broad Lorentzians and a Drude term. For the  $\text{Bi}_2M_{m+1}\text{Co}_m\text{O}_y$  system, the reflectivity increases and assumes a more metallic profile as the number of Co-O layers per unit cell increases, or as the ionic radius of  $M$  increases. The apparent plasma edge of this system is about 0.3 eV, and remains unshifted for all  $\text{Bi}_2M_3\text{Co}_2\text{O}_y$ , as observed in the high- $T_c$  cuprates in which the carrier density is changed by doping. In addition, as observed in the high- $T_c$  cuprates, the reflectivity-frequency profile below the apparent plasma edge is less curved than predicted by the Drude model. For the  $\text{Bi}_2M_{m+1}\text{Co}_m\text{O}_y$  system, the intensity of the mid-ir absorption approximately scales with that of the free-carrierlike absorption. The compounds  $\text{Bi}_2\text{Sr}_3\text{Fe}_2\text{O}_{9.2}$  and  $\text{Bi}_2\text{Sr}_2\text{MnO}_{6.25}$  appear more insulating in reflectivity measurements than does  $\text{Bi}_2M_{m+1}\text{Co}_m\text{O}_y$ . However, the intensity of the mid-ir absorption in these crystals is slightly larger. Our results suggest that the existence of a mid-ir absorption band is not a sufficient condition for the occurrence of high- $T_c$  superconductivity.

## I. INTRODUCTION

The normal-state properties of the high- $T_c$  oxides<sup>1</sup> are not well understood. An example is the frequency dependence of the reflectivity in the mid-ir range, often referred to as the mid-ir absorption. In early studies using ceramic samples, the mid-ir reflectivity was used extensively to identify the plasma edge. A sharp feature in the frequency-dependent conductivity  $\sigma(\omega)$  around 0.5 eV was observed in ceramic samples of  $\text{La}_{2-x}\text{Sr}_x\text{CuO}_{4-y}$  and  $\text{YBa}_2\text{Cu}_3\text{O}_{7-y}$ .<sup>2,3</sup> This was identified with a charge transfer excitation. However, later measurements on single crystals and thin samples of  $\text{YBa}_2\text{Cu}_3\text{O}_{7-y}$  (1:2:3) failed to show the feature near 0.5 eV. Recently, the mid-ir measurements on (1:2:3) by several groups have converged at least qualitatively.<sup>4-8</sup> The free carrier response in the reflectivity has been analyzed in at least two ways, (1) by a Drude model with a frequency-dependent mass and relaxation time or (2) by a Drude-Lorentz model.<sup>4,5,7</sup> Similar spectra were also found in single-crystal  $\text{Bi}_2\text{Sr}_2\text{CuO}_6$ ,<sup>7</sup> in the  $T$ -phase electron-type superconductor  $\text{Nd}_{1.85}\text{Ce}_{0.15}\text{CuO}_{4-8}$ ,<sup>9,10</sup> and in the non-cuprate oxide  $\text{Ba}_{0.6}\text{K}_{0.4}\text{BiO}_3$ .<sup>11</sup> These recent studies have clarified the deviation of  $\sigma(\omega)$  from conventional Drude

behavior, and suggested the existence of an unusual low-frequency excitation. The results could also indicate deviations from conventional normal metal behavior. Although phenomenological models have been proposed, the origin of these deviations is still far from clear.

To further investigate these issues in the high- $T_c$  oxides we have extended reflectivity measurements to the quasi-two-dimensional systems in which Cu in the "bismuthates" is completely replaced by one of the elements Co, Fe, and Mn. At present, very few ir measurements on these systems have been reported.<sup>10</sup> As in the high- $T_c$  Bi-Cu oxides, these compounds undergo a metal-insulator transition upon doping [by changing  $M$  in  $\text{Bi}_2M_3\text{Co}_2\text{O}_y$  ( $y \sim 9.0$ )]. A structural modulation is also induced by insertion of extra oxygen atoms.<sup>12</sup> We compare our results with those of the simple 3d-metal oxides and chalcogenides.

All measurements were performed at room temperature. The reflectivity and the conductivity profiles as derived by a Kramers-Kronig analysis are examined by a Drude-Lorentz model to test the validity of the fit.

## II. EXPERIMENTAL DETAILS

Large crystals (up to  $3 \times 5$  mm<sup>2</sup>) of the single- and double-plane Bi systems (in which Co replaces Cu entire-

ly) were grown at Bellcore using an excess cobalt oxide as the flux.<sup>12,13</sup> In addition to Co substitution for Cu, the alkaline earth metals Ba, Sr, or Ca in  $\text{Bi}_2\text{M}_3\text{Co}_2\text{O}_y$  ( $y \sim 9$ ) were used for  $M$ . The optimum annealing temperature was different for each  $M$ . The compounds  $\text{Bi}_2\text{Sr}_3\text{Fe}_2\text{O}_{9.2}$  (Ref. 14) and  $\text{Bi}_2\text{Sr}_2\text{MnO}_{6.25}$  (Ref. 15) have been obtained also using a 3d-metal oxide as flux but at different growth temperatures. The oxidation states of the 3d metals, inferred from TGA, magnetic susceptibility, and structural data, are  $\sim 3$  in  $\text{Bi}_2\text{M}_3\text{Co}_2\text{O}_y$  ( $M=\text{Ca}, \text{Sr}, \text{Ba}$ ),  $\sim 2.5$  in  $\text{Bi}_2\text{Sr}_2\text{CoO}_{6.25}$ ,  $3-\delta$  in  $\text{Bi}_2\text{Sr}_2\text{MnO}_{6.25}$ , and  $3+\delta$  in  $\text{Bi}_2\text{Sr}_3\text{Fe}_2\text{O}_{9.2}$ . All the Bi oxides were plateletlike and easily cleaved, suggesting weak coupling between adjacent  $ab$  planes. Strong modulation of the Bi atom positions (structural modulation) was detected in all systems by electron and x-ray diffraction measurements.<sup>12</sup> Crystallographic parameters are summarized in Table 1.

None of these systems are superconductors; the compounds  $\text{Bi}_2\text{Sr}_3\text{Fe}_2\text{O}_{9.2}$  (Ref. 14),  $\text{Bi}_2\text{Sr}_2\text{MnO}_{6.25}$ ,  $\text{Bi}_2\text{Sr}_2\text{CoO}_{6.25}$  are insulators. The compound  $\text{Bi}_2\text{Sr}_2\text{MnO}_{6.25}$  is ferrimagnetic with a Néel temperature  $T_N=120$  K, while  $\text{Bi}_2\text{Sr}_2\text{CoO}_{6.25}$  is antiferromagnetic with  $T_N=100-270$  K, depending on the preparation. Further details of sample growth and characterization have been described in Refs. 12–15.

The reflectance was measured at near-normal incidence to the  $ab$  plane of the crystals in a commercial FTIR spectrometer. The surface of the crystals appeared shiny to the eye but significant surface roughness was confirmed by a He-Ne laser diffraction pattern, and, for some crystals, also by optical microscopy. Since the samples were not polished, corrections for surface morphology effects are important in determining the absolute value of the reflectivity of these systems. After measuring the crystals, gold was evaporated onto the crystals and the measurements were repeated. The sample reflectance was normalized to the gold spectrum. Instrumental drift was kept to within a few percent throughout each run. We

estimate that the error in the absolute reflectivity is under 1% between 1000 and 9000  $\text{cm}^{-1}$ . Details of the measurements are described in a previous report.<sup>7</sup>

We carried out a Kramers-Kronig (KK) analysis, using the data at high frequencies (1:2:3,  $\text{La}_{2-x}\text{Sr}_x\text{CuO}_4$  and  $\text{BaPb}_{1-x}\text{Bi}_x\text{O}_3$ ) (Ref. 16) and the ellipsometry data on ceramic samples of  $\text{Bi}_2\text{Sr}_2\text{CoO}_y$ ,  $\text{Bi}_2\text{Sr}_2\text{YCu}_2\text{O}_{8+\delta}$  and  $\text{Bi}_2\text{Sr}_3\text{Fe}_2\text{O}_{9.2}$  (Ref. 17) as extrapolation data at high frequencies.

### III. RESULTS

#### A. $\text{Bi}_2\text{M}_3\text{Co}_2\text{O}_y$ ( $M=\text{Ca}, \text{Sr}, \text{Ba}$ ) and $\text{Bi}_2\text{Sr}_2\text{CoO}_{6.25}$

Figures 1(a) and 1(b) show the typical temperature dependence of the in-plane resistivity  $\rho_{ab}$  and the out-of-plane resistivity  $\rho_c$  of  $\text{Bi}_2\text{Ba}_3\text{Co}_2\text{O}_y$  and  $\text{Bi}_2\text{Ca}_3\text{Co}_2\text{O}_y$ , measured by the Montgomery method,<sup>18</sup> respectively. In general, the system becomes more conducting as the covalent radius of  $M$  in the formula  $\text{Bi}_2\text{M}_3\text{Co}_2\text{O}_y$  becomes larger. In  $\text{Bi}_2\text{Ba}_3\text{Co}_2\text{O}_y$ ,  $\rho_{ab}$  shows a linear  $T$  dependence above 100 K and a sharp increase below 30 K ( $\rho_{ab}=5$  m $\Omega$  cm at 290 K). The out-of-plane resistivity  $\rho_c$  has a quasimetallic temperature dependence, though the resistivity  $\rho_c$  is of the order of  $10^4$  times larger than  $\rho_{ab}$ . In  $\text{Bi}_2\text{Ca}_3\text{Co}_2\text{O}_y$ ,  $\rho_{ab}$  and  $\rho_c$  strongly increase with decreasing  $T$  below 290 K ( $\rho_{ab} \sim 20$   $\Omega$  cm at 290 K). Interestingly,  $\rho_c$  of  $\text{Bi}_2\text{Ca}_3\text{Co}_2\text{O}_y$  at 290 K is smaller than that of  $\text{Bi}_2\text{Ba}_3\text{Co}_2\text{O}_y$ . For the Sr isomorph, a small  $T$  dependence above 100 K is observed, followed by a strong increase below 20 K (Ref. 13) ( $\rho_{ab}$  is a few m $\Omega$  cm at 290 K).  $\rho_{ab}$  in the single-plane variant  $\text{Bi}_2\text{Sr}_2\text{CoO}_{6.25}$  also increases strongly with decreasing  $T$  (Ref. 13) with  $\rho_{ab} \sim 1$   $\Omega$  cm at 290 K. In all these systems, the low- $T$  behavior of  $\rho_{ab}$  can be fitted to the Mott variable range hopping formula.

Figure 2 compares the reflectivity  $R(\omega)$  of the  $\text{Bi}_2\text{M}_{m+1}\text{Co}_m\text{O}_y$  systems. A number of important

TABLE I. Crystallographic parameters of the Bi-3d-metal-based oxides taken from the literature (Refs. 12–15).

	a(Å)	b(Å)	c(Å)	
	(per unit cell)			
$\text{Bi}_2\text{Sr}_2\text{CaCu}_2\text{O}_{8+\delta}$	5.41 (5.39)	5.42 (5.39)	30.9 (30.6)	Ortho
$\text{Bi}_2\text{Sr}_2\text{CuO}_{6+\delta}$	5.38	5.38	24.7	Ortho
$\text{Bi}_2\text{Ca}_3\text{Co}_2\text{O}_y$	4.89	5.06	29.3	Ortho
$\text{Bi}_2\text{Sr}_3\text{Co}_2\text{O}_y$			29.9	Monoclinic
$\text{Bi}_2\text{Ba}_3\text{Co}_2\text{O}_y$			30.8	Monoclinic
$\text{Bi}_2\text{Sr}_2\text{CoO}_{6.25}$	5.46	5.47	23.5	Ortho
$\text{Bi}_2\text{Sr}_3\text{Fe}_2\text{O}_{9.2}$	5.45	5.46	31.7	Ortho
$\text{Bi}_2\text{Sr}_2\text{MnO}_{6.25}$	5.45	5.43	23.6	Ortho

features are obvious below  $2000\text{ cm}^{-1}$ . The overall reflectivity  $R(\omega)$  tends to be higher for the larger  $M$ 's (Ba). Compounds with large  $M$  are more conductive, as will become apparent in a Kramers-Kronig analysis. Moreover, in the reflectivity of  $\text{Bi}_2\text{Sr}_{m+1}\text{Co}_m\text{O}_y$ , the single Co-O layer compound ( $m=1$ ) appears more insulating than the double Co-O layer compound ( $m=2$ ). These trends agree qualitatively with the dc resistivity results. However, the *apparent* plasma edge remains near  $2500\text{ cm}^{-1}$  ( $0.3\text{ eV}$ ). Similar behavior has been observed as well in the Cu-O based high- $T_c$  systems. When  $\text{La}_2\text{CuO}_4$  is doped with Sr, the Drude-like reflectivity increases but the apparent plasma edge always stays near  $1\text{ eV}$ .<sup>19</sup> Similar observations in  $\text{YBa}_2\text{Cu}_3\text{O}_{6+x}$ ,<sup>8</sup> ceramic  $\text{Bi}_2\text{Sr}_{2-x}\text{Ca}_{x+n-1}\text{Cu}_n\text{O}_y$ ,<sup>20</sup>  $\text{Nd}_{2-x}\text{Ce}_x\text{CuO}_{4-8}$ ,<sup>21</sup> and the noncuprate system  $\text{BaPb}_{1-x}\text{Bi}_x\text{O}_3$  (Ref. 22) have been reported, and frequently interpreted in terms of the mid-ir absorption.<sup>4,5,7-9</sup> We may also assume the existence of an absorption band below  $0.3\text{ eV}$  in analyzing the spectra of the  $\text{Bi}_2\text{M}_3\text{Co}_2\text{O}_y$  systems. In the next two paragraphs, we discuss the reflectivity  $R(\omega)$  of the  $\text{Bi}_2\text{M}_{m+1}\text{Co}_m\text{O}_y$  systems below  $0.3\text{ eV}$ .

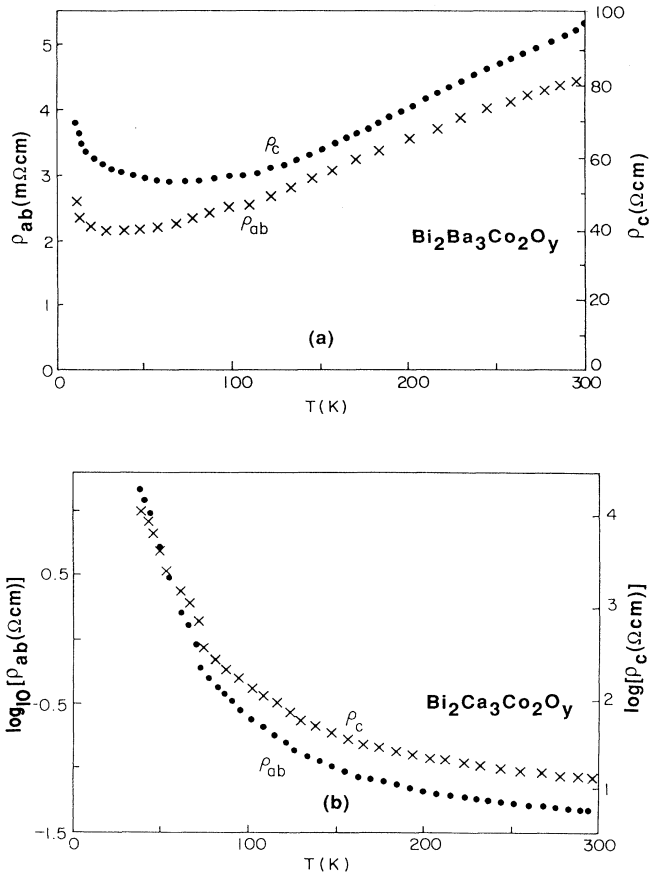


FIG. 1. Temperature dependence of the in-plane resistivity ( $\rho_{ab}$ ) and the out-of-plane resistivity ( $\rho_c$ ) of  $\text{Bi}_2\text{Ba}_3\text{Co}_2\text{O}_y$  (a) and  $\text{Bi}_2\text{Ca}_3\text{Co}_2\text{O}_y$  (b).

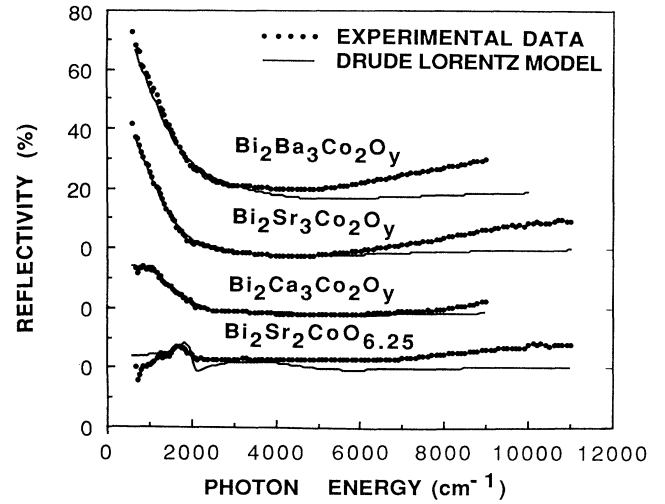


FIG. 2. Measured reflectivity of  $\text{Bi}_2\text{Ba}_3\text{Co}_2\text{O}_y$ ,  $\text{Bi}_2\text{Sr}_3\text{Co}_2\text{O}_y$ ,  $\text{Bi}_2\text{Ca}_3\text{Co}_2\text{O}_y$ , and  $\text{Bi}_2\text{Sr}_2\text{CoO}_{6.25}$  (dots), and Drude-Lorentz model fits [Eq. (3)] (solid lines).

First, we attempted a fit of  $R(\omega)$  of  $\text{Bi}_2\text{M}_3\text{Co}_2\text{O}_y$  ( $M=\text{Ba, Sr}$ ) with a Drude model alone,

$$\epsilon = \epsilon_\infty - \omega_p^2 / [(\omega + i\tau^{-1})\omega] \quad (1)$$

between  $600$  and  $2000\text{ cm}^{-1}$  ( $\omega$ : frequency of the incident light) (Fig. 3). Fitting parameters used are listed in Table II. The fit is unsatisfactory and the fitting parameters are not physically reasonable. However, as shown in  $\text{La}_{2-x}\text{Sr}_x\text{CuO}_4$ ,<sup>19</sup> the change of the plasma frequency  $\omega_p$  is small and the scattering rate  $\tau^{-1}$  decreases with doping (i.e., with a larger  $M$ ). [In Table II, the carrier density  $n$

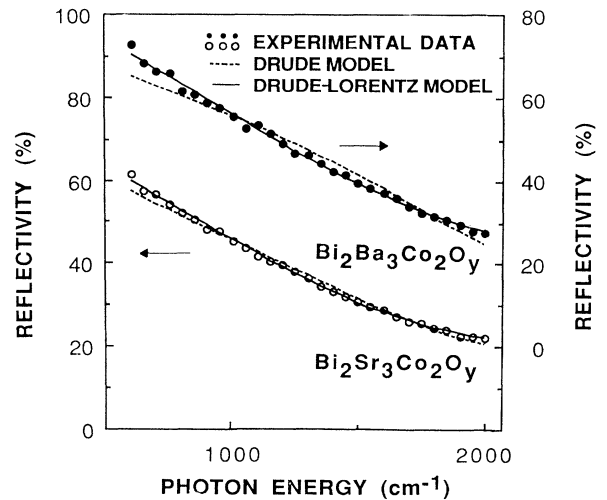


FIG. 3. Fit by a Drude model [Eq. (1)] (dashed lines) and by a Drude Lorentz model [Eq. (2)] to the measured reflectivity of  $\text{Bi}_2\text{Ba}_3\text{Co}_2\text{O}_y$  (solid circles) and  $\text{Bi}_2\text{Sr}_3\text{Co}_2\text{O}_y$  (open circles).

TABLE II. Fit parameters for a Drude model [Eq. (1)] and for a Drude model with frequency-dependent scattering rate ( $\tau^{-1} = \tau_0^{-1} + \alpha\omega$ ) (in parentheses) to the reflectivity of  $\text{Bi}_2\text{Ba}_3\text{Co}_2\text{O}_y$  and  $\text{Bi}_2\text{Sr}_3\text{Co}_2\text{O}_y$ .

	$\omega_p$ ( $\text{cm}^{-1}$ )	$\tau_0^{-1}$ ( $\text{cm}^{-1}$ )	$\alpha$	$\epsilon_\infty$	$\rho_{\text{DC}}$ ( $\text{m}\Omega \text{ cm}$ )	$\rho_{ab}$	$\hbar\tau_0^{-1}$ ( $k_B T$ )	$n$ ( $m^*/m \text{ cm}^{-3}$ )
$\text{Bi}_2\text{Ca}_3\text{Co}_2\text{O}_y$	1200	3100		7	130	20	14.6	$0.2 \times 10^{20}$
$\text{Bi}_2\text{Sr}_3\text{Co}_2\text{O}_y$	5700 (6300)	2000 1600	0.8	7 7	4 2		9.5 6.7	$3.6 \times 10^{20}$ $4.5 \times 10^{20}$
$\text{Bi}_2\text{Ba}_3\text{Co}_2\text{O}_y$	6100 (8600)	1600 900	2.1	7 7	3 1	5	7.6 3.8	$4.1 \times 10^{20}$ $8.3 \times 10^{20}$

and the dc resistivity ( $\rho_{\text{dc}}$ ) estimated from the Drude parameters are also listed together with the resistivity  $\rho_{ab}$  obtained from transport measurements.]

In  $\text{Bi}_2\text{Ba}_3\text{Co}_2\text{O}_y$  and  $\text{Bi}_2\text{Sr}_3\text{Co}_2\text{O}_y$ , the Drude fit to  $R(\omega)$  deviates from the data in a way very similar to that observed in several high- $T_c$  cuprates such as (1:2:3),  $\text{Bi}_2\text{Sr}_2\text{CuO}_{6+\delta}$ ,<sup>7</sup> and  $\text{Nd}_{2-x}\text{Ce}_x\text{CuO}_{4-\delta}$ .<sup>9</sup> In particular, the  $R(\omega) - \omega$  profile calculated from the Drude fit is more curved than the measured reflectivity. As in the case of the high- $T_c$  cuprate,<sup>4,6,7,9</sup> this difference can be reduced by inclusion of a Lorentz oscillator below 0.3 eV ( $2400 \text{ cm}^{-1}$ ) or by a Drude model with a frequency-dependent  $\tau^{-1}$ . In Fig. 3 we show fits to a Drude-Lorentz model (DL model):

$$\epsilon = \epsilon_\infty - \omega_p^2 / [(\omega + i\tau^{-1})\omega] - \omega_{pl}^2 / (\omega^2 - \omega_r^2 + i\omega\tau_l^{-1}). \quad (2)$$

The DL fit parameters ( $\omega_p, \tau^{-1}, \omega_{pl}, \tau_l^{-1}, \omega_r$ ) are listed in Table III. As shown in the high- $T_c$  cuprates,<sup>8,21</sup> the peak intensity of the Lorentz oscillator in the conductivity  $\sigma(\omega)$  ( $\omega_{pl}^2 / \tau_l^{-1}$ ) scales with that of the Drude term ( $\omega_p^2 / \tau^{-1}$ ). A Drude model with a frequency-dependent scattering rate  $\tau^{-1} = \tau_0^{-1} + \alpha\omega$  fits the reflectivity equally well as the DL model. The fit parameters are also listed in the parentheses in Table II. Throughout, we reserve the term ‘‘mid-ir absorption’’ for the spectral range near 0.5 eV (as distinct from the 0.2-eV range).

We fitted  $R(\omega)$  between 600 and  $9000 \text{ cm}^{-1}$  with a

Drude model. The fit was unsatisfactory and required very large  $\epsilon_\infty (> 10)$ , which may suggest that at least one broad, Lorentzian-like term in the mid- or near-ir range needs to be included in the model to fit  $R(\omega)$  between 600 and  $9000 \text{ cm}^{-1}$ .

In order to investigate the spectrum further, especially near 0.5 eV, we carried out a Kramers-Kronig analysis (KK). Figure 4 shows the frequency-dependent conductivity  $\sigma(\omega)$  for  $\text{Bi}_2\text{M}_{m+1}\text{Co}_m\text{O}_y$ . First we focus on the broad structure between 2000 and  $6000 \text{ cm}^{-1}$ . The more conductive system (or a system with higher reflectivity at low  $\omega$ ) seems to show a more intense mid-ir absorption. The overall values of  $\sigma(\omega)$  are much smaller than those of the high- $T_c$  cuprates. [ $\sigma(\omega)$  for  $\text{Bi}_2\text{Ba}_3\text{Co}_2\text{O}_y$  ( $200 \Omega^{-1} \text{ cm}^{-1}$ ) near  $4000 \text{ cm}^{-1}$  is only 40% of that in  $\text{Bi}_2\text{Sr}_2\text{CuO}_{6+\delta}$ .<sup>10</sup> Recent results on  $\text{YBa}_2\text{Cu}_3\text{O}_{6+x}$  with different doping concentrations ( $x$ ) show a similar dependence of the mid-ir absorption intensity on the free carrier absorption.<sup>8</sup> Although the shape of the absorption differs slightly from Lorentzian, we fitted  $R(\omega)$  between 600 and  $6000 \text{ cm}^{-1}$  to a DL model having two Lorentzians,

$$\epsilon = \epsilon_\infty - \omega_p^2 / [(\omega + i\tau^{-1})\omega] - \omega_{pl}^2 / (\omega^2 - \omega_r^2 + i\omega\tau_l^{-1}) - \omega_{pm}^2 / (\omega^2 - \omega_{rm}^2 + i\omega\tau_m^{-1}). \quad (3)$$

The DL fit parameters are given in Table III. As shown

TABLE III. Tentative fit parameters for a Drude Lorentz model [Eqs. (2), (3), and (4)] to the reflectivity between  $650\text{--}6000 \text{ cm}^{-1}$ . Lorentz model fit parameters for the phonon ( $\omega_{pn}, \tau_n^{-1}, \omega_{rm}$ ) are not listed. The fit parameters in parentheses are those for the fit where  $\epsilon_\infty = 7$  is given.

	$\omega_{pl}$	$\tau_l^{-1}$	$\omega_r$	$\omega_{pn}$	$\tau_m^{-1}$ ( $\text{cm}^{-1}$ )	$\omega_{rm}$	$\omega_p$	$\tau^{-1}$	$\epsilon_\infty$
$\text{Bi}_2\text{Ba}_3\text{Co}_2\text{O}_y$	7100	4300	800	4500	5200	(4000)	3400	400	7
$\text{Bi}_2\text{Sr}_3\text{Co}_2\text{O}_y$	5900	4400	1300	2800	3600	(4000)	3300	600	7
$\text{Bi}_2\text{Ca}_3\text{Co}_2\text{O}_y$	4100 (4100)	2200 2200	1500 1500	3800 1800	4000 1400	4900 3800	1200 1200	3100 3100	6.5 7)
$\text{Bi}_2\text{Sr}_2\text{CoO}_{6.25}$	1600	300	2000	3900	2800	(4500)			6.9
$\text{Bi}_2\text{Sr}_2\text{MnO}_{6.25}$	3200	500	2000	9400	5100	5200			7
$\text{Bi}_2\text{Sr}_3\text{Fe}_2\text{O}_{9.2}$	1500	700	3200	29 000	13 000	13 000			4

in Figs. 2 and 4 the DL fits deviate from the measured  $R(\omega)$  and  $\sigma(\omega)$  at higher frequencies, and  $R(\omega)$  slowly increases with photon energy ( $\omega$ ), as is most easily seen in  $\sigma(\omega)$  of  $\text{Bi}_2\text{Sr}_2\text{CoO}_{6.25}$ . These results suggest that an additional Lorentz oscillator above 1 eV is necessary as long as a DL model is applied. But it is difficult to fit both  $R(\omega)$  and  $\sigma(\omega)$  by a DL or a Lorentz model with a Lorentzian near 1.5 eV but without a Lorentzian near 0.5 eV. In summary, a DL model would need a Drude term and at least three Lorentzian oscillators (one below 0.3 eV, one around 0.4–0.6 eV, one above 1 eV) in order to fit  $R(\omega)$  and  $\sigma(\omega)$  adequately between 0.08 and 1.4 eV.

A relatively clear structure below  $2000\text{ cm}^{-1}$  is observed in  $R(\omega)$  and  $\sigma(\omega)$  of  $\text{Bi}_2\text{Sr}_2\text{CoO}_{6.25}$ . In  $\text{Bi}_2\text{Ca}_3\text{Co}_2\text{O}_y$ , this structure obscures the small Drude-like component in  $R(\omega)$  and  $\sigma(\omega)$ . This absorption may account for the deviation from the Drude model mentioned above. Further discussion of this feature will be given when we describe the results on  $\text{Bi}_2\text{Sr}_2\text{MnO}_{6.25}$  and  $\text{Bi}_2\text{Sr}_3\text{Fe}_2\text{O}_{9.2}$  in the next section.

### B. $\text{Bi}_2\text{Sr}_2\text{MnO}_{6.25}$ and $\text{Bi}_2\text{Sr}_3\text{Fe}_2\text{O}_{9.2}$

In order to study the effect of substitution of Cu by other 3d metals we performed similar measurements on

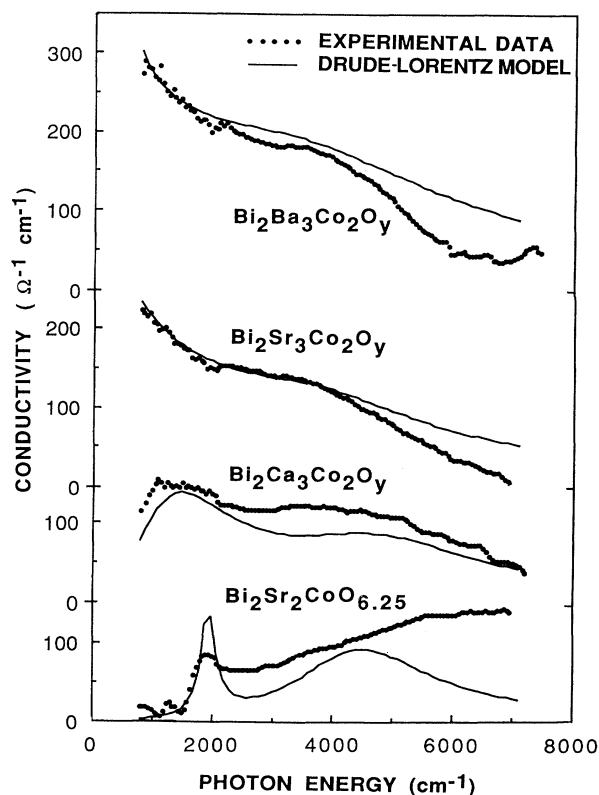


FIG. 4. Conductivity  $\sigma(\omega)$  of  $\text{Bi}_2\text{Ba}_3\text{Co}_2\text{O}_y$ ,  $\text{Bi}_2\text{Sr}_3\text{Co}_2\text{O}_y$ ,  $\text{Bi}_2\text{Ca}_3\text{Co}_2\text{O}_y$ , and  $\text{Bi}_2\text{Sr}_2\text{CoO}_{6.25}$  derived by a KK analysis (dots) and Drude-Lorentz model fits [Eq. (3)] (solid lines).

$\text{Bi}_2\text{Sr}_2\text{MnO}_{6.25}$  and  $\text{Bi}_2\text{Sr}_3\text{Fe}_2\text{O}_{9.2}$ . Unfortunately, because we could not obtain single-phased  $\text{Bi}_2\text{Sr}_2\text{FeO}_y$ ,<sup>12</sup> we investigated  $\text{Bi}_2\text{Sr}_3\text{Fe}_2\text{O}_{9.2}$  instead. Figure 5 shows the reflectivity  $R(\omega)$  of these oxides. Indicative of the strongly insulating nature of the compounds, a prominent unscreened phonon peak is observed near  $620\text{ cm}^{-1}$ . This phonon is assigned to the Mn-O or Fe-O stretch mode in analogy with the Cu-O system.<sup>23,24</sup> The intensity of the phonon line is unexpectedly high. This may be due to the large ambiguity (on the order of 10%) in the absolute reflectivity below  $1000\text{ cm}^{-1}$  [the beam splitter used (KCl) has a cut-off frequency at  $550\text{ cm}^{-1}$ ]. Therefore, we do not discuss the phonon structure in detail.

Figure 6 shows the KK results. In both  $R(\omega)$  and  $\sigma(\omega)$ , a hump around  $2000\text{ cm}^{-1}$  is evident. In the literature on the optical reflectivity of the Mn chalcogenides [MnS (Ref. 25) and MnSe (Ref. 26)], no clear structure near 0.3 eV is reported. We have measured only two samples from the same batch, but, nonetheless, analytical work on our crystals rules out an extrinsic impurity effect. A similar broad structure is also observed in  $\text{Bi}_2\text{Sr}_2\text{CoO}_{6.25}$ , which was measured several times by cleaving the sample surface repeatedly. The evidence indicates that this feature is real. A corresponding structure is not discernible in the insulating phases of the high- $T_c$  cuprates [(1:2:3),<sup>8</sup>  $\text{La}_{2-x}\text{Sr}_x\text{CuO}_y$ ,<sup>6</sup>  $\text{Bi}_2\text{Sr}_2$  (Ca, Nd)  $\text{Cu}_2\text{O}_{8+\delta}$  (Ref. 27)]. The hump structure which we observe in the series  $\text{Bi}_2\text{M}_{m+1}\text{R}_m\text{O}_y$  ( $R=\text{Co, Fe, Mn}$ ,  $m=1,2$ ), apparently becomes more well defined as the atomic number of  $R$  decreases. In  $\text{Bi}_2\text{Ca}_3\text{Co}_2\text{O}_y$ , the magnitude of the hump may be enhanced by a free carrier contribution.

Finally we discuss the absorption centered around 0.5 eV and the overall structure. The  $R(\omega)-\omega$  profile mea-

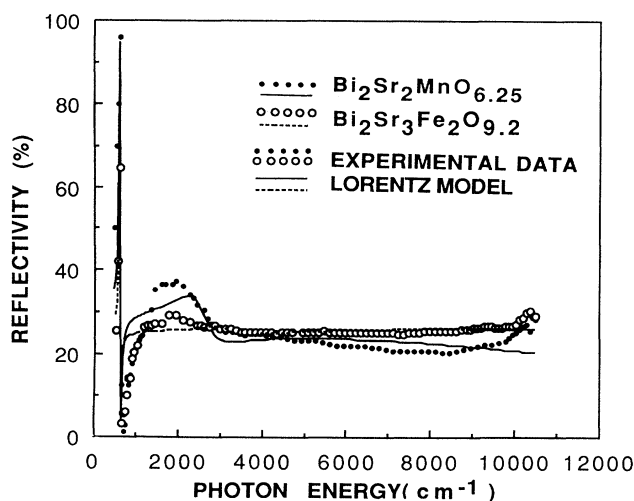


FIG. 5. Measured reflectivity of  $\text{Bi}_2\text{Sr}_3\text{Fe}_2\text{O}_{9.2}$  (open circles) with a Lorentz model fit [Eq. (4)] (dashed line), and the measured reflectivity of  $\text{Bi}_2\text{Sr}_2\text{MnO}_{6.25}$  (dots) with a Lorentz model fit (solid line).

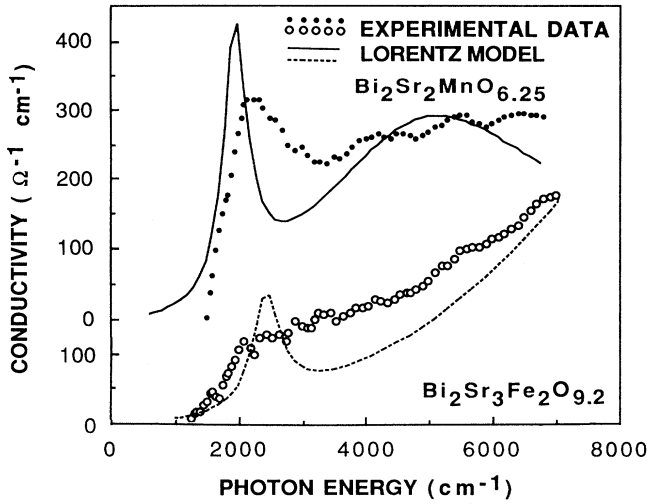


FIG. 6. Conductivity  $\sigma(\omega)$  of  $\text{Bi}_2\text{Sr}_3\text{Fe}_2\text{O}_{9.2}$  (open circles) with a Lorentz model fit [Eq. (4)] (dashed line), and the conductivity  $\sigma(\omega)$  of  $\text{Bi}_2\text{Sr}_2\text{MnO}_{6.25}$  (dots) and a Lorentz model fit (solid line).

sured here is very similar to that of the Mott insulators NiO (Ref. 28) and  $\text{CoO}$ ,<sup>29</sup> and to that of Mn chalcogenides<sup>25,26</sup> (with the exception of the hump discussed above). However, unlike these simple insulators, a mid-ir absorption is clearly observed in our samples. The intensity of the absorption in the mid-ir range in  $\text{Bi}_2\text{Sr}_2\text{MnO}_{6.25}$  and  $\text{Bi}_2\text{Sr}_3\text{Fe}_2\text{O}_{9.2}$  is higher than that in  $\text{Bi}_2\text{Sr}_3\text{Co}_2\text{O}_y$  and  $\text{Bi}_2\text{Ba}_3\text{Co}_2\text{O}_y$  which are metallic at room temperature and have significant free carrier absorption. When  $\text{Bi}_2\text{M}_{m+1}\text{Co}_m\text{O}_y$ ,  $\text{YBa}_2\text{Cu}_3\text{O}_{6+x}$ ,<sup>8</sup> or  $\text{Bi}_2\text{Sr}_2(\text{Ca}_{1-x}\text{Nd}_x)\text{Cu}_2\text{O}_{8+\delta}$  (Ref. 27) is chemically doped (by changing  $M$  or  $x$ ), a positive correlation between the intensity of free carrier absorption and that of the mid-ir absorption is found. We can also induce a conductor to insulator transition in  $\text{Bi}_2\text{Sr}_{m+1}\text{Cu}_m\text{O}_y$  by substituting  $R$  ( $=\text{Co}, \text{Fe}, \text{Mn}$ ) for Cu instead of changing Sr or the O content ( $y$ ). However, the above correlation disappears when the system is made insulating by replacing Cu with R.

The reflectivity between 600 and 6000  $\text{cm}^{-1}$  is fitted with a Lorentz model,

$$\epsilon = \epsilon_\infty - \frac{\omega_{pl}^2}{(\omega^2 - \omega_r^2 + i\omega\tau_l^{-1})} - \frac{\omega_{pm}^2}{(\omega^2 - \omega_{rm}^2 + i\omega\tau_m^{-1})} - \frac{\omega_{pn}^2}{(\omega^2 - \omega_{rn}^2 + i\omega\tau_n^{-1})}, \quad (4)$$

where the first, second, and third oscillators represent the hump, a mid-ir absorption, and phonon, respectively. The  $\sigma(\omega)$  calculated from a Lorentz model along with the parameters obtained is also shown in Fig. 6. The fit parameters ( $\omega_{pl}$ ,  $\omega_r$ ,  $\tau_l^{-1}$ ,  $\omega_{pm}$ ,  $\omega_{rm}$ ,  $\tau_m^{-1}$ ) are listed in Table III.

Both  $R(\omega)$  and  $\sigma(\omega)$  of  $\text{Bi}_2\text{Sr}_3\text{Fe}_2\text{O}_{9.2}$  tend to increase with the photon energy  $\omega$ . This suggests that an additional oscillator is needed above 1 eV. Actually, as shown in Table III, the Lorentz oscillator at the highest

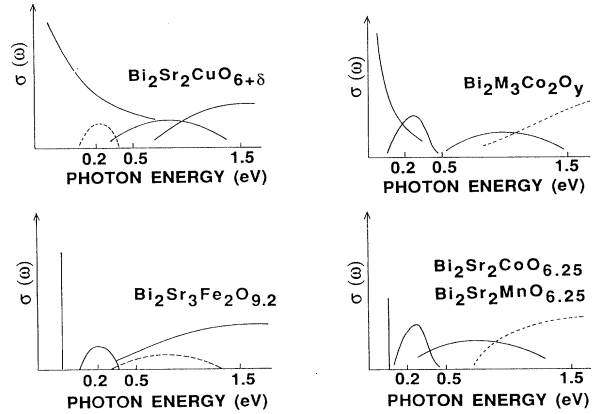


FIG. 7. Summary of the model fits, showing the contribution of each term in a Drude-Lorentz model to the ac conductivity  $\sigma(\omega)$ . The dashed lines in the sketches for  $\text{Bi}_2\text{Sr}_3\text{Fe}_2\text{O}_{9.2}$  and  $\text{Bi}_2\text{Sr}_2\text{CuO}_{6+\delta}$  shows speculated absorption bands.

frequency is not located in the mid-ir range. With its center frequency moved up to 1.5 eV, the oscillator improves the fit to  $R(\omega)$  and  $\sigma(\omega)$ , but the overall fit remains unsatisfactory. Similarly, in  $\text{Bi}_2\text{Sr}_2\text{MnO}_{6.25}$ , the DL fits (without an extra oscillator above 1 eV) are always smaller than  $R(\omega)$  and  $\sigma(\omega)$  at high frequencies. This suggests that an extra oscillator above 1 eV is also needed in this compound.

In summary, we could identify two absorption bands near 0.3 and 0.5 eV, probably because the apparent plasma edge is located at frequencies much lower than those in high- $T_c$  cuprates. The reflectivity of  $\text{Bi}_2\text{M}_{m+1}\text{R}_m\text{O}_y$  [ $M=\text{Ca}, \text{Sr}, \text{Ba}$ ,  $R=3d\text{-metal}$  ( $\text{Co}, \text{Fe}, \text{Mn}$ ),  $x=1,2$ ] in the mid- and near-ir range is described by three broad absorption bands (one near 0.2~0.3 eV, one near 0.5 eV, and one above 1.0 eV) and a free carrier response (in case of the metallic samples). We speculate that this may be true as well in the Bi-Cu system, possibly with a much smaller absorption near 0.3 eV. We summarize these conclusions in Fig. 7.

#### IV. DISCUSSION

The mid-ir absorption has been discussed in connection with the mechanism of high- $T_c$  superconductivity<sup>30</sup> and with the transfer of spectral weight from the charge-transfer gap.<sup>21,31,32</sup> There is also evidence for a rough positive correlation between the maximum  $T_c$  of a given system and the location of the apparent plasma edge, including the present results (nonsuperconductor). However, we are skeptical about a direct connection between the mid-ir absorption and the high- $T_c$  mechanism, because (1) a positive correlation between the mid-ir absorption and the free carrier absorption is also observed in the nonsuperconducting system ( $\text{Bi}_2\text{M}_{m+1}\text{Co}_m\text{O}_y$ ) and (2) the mid-ir absorption is also found in the insulator  $\text{Bi}_2\text{Sr}_2\text{MnO}_{6.25}$ , with a magnitude similar to the high- $T_c$  Bi-Cu oxides.<sup>10,27</sup>

The  $\sigma(\omega)$ - $\omega$  profile of  $\text{Bi}_2\text{Sr}_3\text{Fe}_2\text{O}_{9.2}$  seems qualitatively

different from the other insulators studied here;  $\sigma(\omega)$  of  $\text{Bi}_2\text{Sr}_3\text{Fe}_2\text{O}_{9.2}$  increases steadily with  $\omega$ . While  $\text{Bi}_2\text{Sr}_2\text{MnO}_{6.25}$  and  $\text{Bi}_2\text{Sr}_2\text{CoO}_{6.25}$  exhibit oxygen disorder or oxygen vacancy in the Bi-O plane,  $\text{Bi}_2\text{Sr}_3\text{Fe}_2\text{O}_{9.2}$  does not.<sup>12</sup> This may account for the above difference in  $\sigma(\omega)$ . This idea is supported by the previous observations of a mid-ir absorption band in  $\text{SrTiO}_3$  and  $\text{BaTiO}_3$ . In Ref. 33 this band was attributed to deep impurity states associated with oxygen vacancies.

As we discussed above, the free carrierlike absorption and the mid-ir absorption have been well correlated in the several quasi-two-dimensional cuprates and cobalt oxides related with high- $T_c$  superconductors. An absorption band similar to the mid-ir absorption is also observed in the 3d-metal chalcogenides which show a metal-insulator transition.<sup>34–36</sup> In NiO, which does not undergo a metal-insulator transition, the intensity of a broad mid-ir absorption between 0.2 and 1 eV is enhanced by doping and thus positively correlated with carrier density, though the intensity of the absorption was very weak.<sup>28</sup> These observations suggest that the mid-ir absorption may be related with a general property of the metal-insulator transition.

In this paper we have referred to the absorption near 0.5 eV as the mid-ir absorption. However, it is also possible to regard the absorption band below 0.3 eV in  $\text{Bi}_2\text{M}_3\text{Co}_2\text{O}_y$  as the mid-ir absorption band directly analogous to that observed in the high- $T_c$  cuprates, and to treat the 0.5-eV band in the former as a new absorption feature. We are less comfortable with this viewpoint, since it regards the cuprates as a special class of materials distinct from other oxides R-O systems ( $R = \text{Co}, \text{Fe}, \text{Mn}$ ).

## V. CONCLUSION

A broad absorption in the mid-ir range was observed in all crystals of the quasi-two-dimensional oxides studied,

including  $\text{Bi}_2\text{Sr}_2\text{MnO}_{6.25}$ , a good insulator.

The apparent plasma edge of  $\text{Bi}_2\text{M}_3\text{Co}_2\text{O}_y$  is located at  $\sim 0.3$  eV, which is about one-third of that of  $\text{Bi}_2\text{Sr}_2(\text{Ca}, \text{Nd})\text{Cu}_2\text{O}_y$ .<sup>27</sup> In comparison with the reflectivity in the cuprates, the much lower plasma edge in the former compounds allows the identification of two absorption bands below 1 eV. In order to fit the observed reflectivity with a Drude-Lorentz model, three oscillators are required (one below 0.3 eV, one at 0.5–0.7 eV, and one above 1 eV). (The case of  $\text{Bi}_2\text{Sr}_3\text{Fe}_2\text{O}_{9.2}$  is an exception.) In the case of  $\text{Bi}_2\text{M}_3\text{Co}_2\text{O}_y$  ( $M = \text{Ba}, \text{Sr}$ ), the low-frequency reflectivity may also be described by a Drude model with a frequency-dependent scattering rate, in place of the oscillator below 0.3 eV.

The nonsuperconductors  $\text{Bi}_2\text{M}_{m+1}\text{Co}_m\text{O}_y$  show striking similarities to the Cu-O high- $T_c$  oxides, such as a correlation of a Drude-like reflectivity with the intensity of the mid-ir absorption, the insensitivity of the apparent plasma edge to the doping level, and a frequency-reflectivity profile more linear than that calculated from a Drude model.

These results suggest that the existence of a mid-ir absorption band is not a sufficient condition for the occurrence of the high- $T_c$  superconductivity. It appears to be present in several classes of 3d-metal oxides, especially those that undergo a metal-insulator transition. In addition, a new hump structure was observed in the insulating samples of  $\text{Bi}_2\text{M}_{m+1}\text{R}_m\text{O}_y$  ( $R = \text{Co}, \text{Fe}, \text{Mn}$ ).

## ACKNOWLEDGMENTS

We thank Dr. S. Uchida, Dr. S. A. Lyon, and Dr. G. A. Thomas for many helpful discussions. Y.W. acknowledges support from Mitsubishi Kasei (Japan). This work was supported in part by the Office of Naval Research (Contract Nos. N00014-90-J-1013 and N0014-89-J-1567).

\*Present address: Mitsubishi Kasei Research Center, Midori-ku Yokohama 227, Japan.

<sup>1</sup>J. G. Bednorz and K. A. Muller, *Z. Phys. B* **64**, 189 (1986).

<sup>2</sup>K. Kamaras, C. D. Porter, M. G. Doss, S. L. Herr, D. B. Tanner, D. A. Bonn, J. E. Greedan, A. H. O'Reilly, C. V. Stager, and T. Timusk, *Phys. Rev. Lett.* **59**, 919 (1987).

<sup>3</sup>J. Orenstein, G. A. Thomas, D. H. Rapkine, C. B. Bethea, B. F. Levine, R. J. Cava, E. A. Reitman, and D. W. Johnson, Jr., *Phys. Rev. B* **36**, 729 (1987).

<sup>4</sup>G. A. Thomas, J. Orenstein, D. H. Rapkine, and M. Capizzi, A. J. Millis, R. N. Bhatt, L. F. Schneemeyer, and J. V. Waszczak, *Phys. Rev. Lett.* **61**, 1313 (1988).

<sup>5</sup>T. Timusk, S. L. Herr, K. Kamaras, C. D. Porter, D. B. Tanner, D. A. Bonn, J. D. Garrett, C. V. Stager, J. E. Greedan, and M. Reedyk, *Phys. Rev. B* **38**, 6683 (1988).

<sup>6</sup>R. T. Collins, Z. Schlesinger, F. Holtzberg, P. Chaudari, and C. Field, *Phys. Rev. B* **39**, 6571 (1989).

<sup>7</sup>Y. Watanabe, Z. Z. Wang, S. A. Lyon, D. C. Tsui, N. P. Ong, J. M. Tarascon, and P. Barboux, *Phys. Rev. B* **40**, 6884 (1989).

<sup>8</sup>J. Orenstein, G. A. Thomas, A. J. Millis, S. L. Cooper, D. H. Rapkine, T. Timusk, L. F. Schneemeyer, and J. V. Waszczak, *Phys. Rev. B* **42**, 6342 (1990).

<sup>9</sup>Y. Watanabe, Z. Z. Wang, S. A. Lyon, D. C. Tsui, N. P. Ong, J. M. Tarascon, and E. Wang, *Solid State Commun.* **74**, 757 (1990).

<sup>10</sup>Y. Watanabe, Z. Z. Wang, S. A. Lyon, D. C. Tsui, N. P. Ong, J. M. Tarascon, P. Barboux, and E. Wang, in *Physics and Materials Science of High Temperature Superconductors*, Vol. 181 of *NATO Advanced Study Institute, Series E: Applied Sciences*, edited by R. Kossowsky *et al.* (Kluwer Academic, Dordrecht, 1990), p. 429.

<sup>11</sup>Z. Schlesinger, R. T. Collins, J. A. Calise, D. G. Hinks, A. W. Mitchell, Y. Zheng, B. Dabrowski, N. E. Bickers, and D. J. Scalapino, *Phys. Rev. B* **40**, 6862 (1989).

<sup>12</sup>J. M. Tarascon, P. F. Miceli, P. Barboux, D. M. Hwang, G. W. Hull, M. Giroud, L. H. Greene, Y. LePage, W. R. Mckinnon, E. Tselepis, G. Pleizier, E. Eibscutz, D. A. Neumann, and J. J. Rhyne, *Phys. Rev. B* **39**, 11587 (1989); J. M. Tarascon, Y. LePage, W. R. Mckinnon, E. Tselepis, P. Barboux, B. G. Bagley, and R. Ramesh, in *High Temperature Superconductors: Relationships Between Properties, Structure, and Solid-State Chemistry*, MRS Symposia Proceedings No. 156 (Materials Research Society, Pittsburgh, 1989), p. 317.

<sup>13</sup>J. M. Tarascon, R. Ramesh, P. Barboux, M. S. Hedge, G. W.



- Hull, L. H. Greene, M. Giroud, Y. LePage, W. R. Mckinnon, J. V. Waszczak, and L. F. Schneemeyer, *Solid State Commun.* **71**, 663 (1989).
- <sup>14</sup>Y. Lepage, W. R. Mckinnon, J. M. Tarascon, and P. Barbour, *Phys. Rev. B* **40**, 6810 (1989).
- <sup>15</sup>W. R. Mckinnon, E. Tselepis, Y. LePage, S. P. McAlister, G. Pleizier, J. M. Tarascon, P. F. Miceli, R. Ramesh, G. W. Hull, J. V. Waszczak, E. J. J. Rhyne, and D. A. Neumann, *Phys. Rev. B* **41**, 4489 (1990).
- <sup>16</sup>H. Ishii, I. Rittaporn, H. Takagi, S. Tajima, S. Uchida, S. Tanaka, M. Suzuki, T. Murakami, M. Seki, and S. Suga, *Physica C* **153-155**, 655 (1988).
- <sup>17</sup>M. K. Kelly, P. Barbour, J. M. Tarascon, and D. E. Aspnes, *Phys. Rev. B* **40**, 6797 (1989).
- <sup>18</sup>H. C. Montgomery, *J. Appl. Phys.* **42**, 2971 (1971).
- <sup>19</sup>M. Suzuki, *Phys. Rev. B* **39**, 2312 (1989).
- <sup>20</sup>A. Maeda, M. Hase, I. Tsukada, K. Noda, S. Taebayashi, and K. Uchinokura, *Phys. Rev. B* **41**, 6418 (1990).
- <sup>21</sup>T. Tokura, T. Arima, S. Koshihara, T. Ido, S. Ishibashi, H. Takagi, and S. Uchida, in *Advances in Superconductivity II* (ISS'89), 51 (Springer-Verlag, Tokyo, 1990).
- <sup>22</sup>S. Tajima, S. Uchida, A. Masaki, H. Takagi, K. Kitazawa, S. Tanaka, and A. Katsui, *Phys. Rev.* **32**, 6302 (1985).
- <sup>23</sup>M. K. Crawford, G. Burns, and F. Holtzberg, *Solid State Commun.* **70**, 557 (1989).
- <sup>24</sup>S. Tajima, S. Uchida, S. Ishibashi, T. Ido, H. Takagi, T. Arima, and Y. Tokura, *Physica C* **168**, 117 (1990).
- <sup>25</sup>D. R. Huffman and R. L. Wild, *Phys. Rev.* **156**, 989 (1967).
- <sup>26</sup>D. L. Decker and R. L. Wild, *Phys. Rev. B* **4**, 3425 (1971).
- <sup>27</sup>I. Terasaki, T. Nakanishi, S. Takebayashi, A. Maeda, and K. Uchinokura, *Physica C* **165**, 152 (1990).
- <sup>28</sup>R. Newman and R. M. Chrenko, *Phys. Rev.* **114**, 1507 (1959).
- <sup>29</sup>R. J. Powell and W. E. Spicer, *Phys. Rev. B* **2**, 2182 (1970).
- <sup>30</sup>As examples, C. M. Varma, P. B. Littlewood, S. Scmitt-Rink, E. Abrahams, and A. E. Ruckenstein, *Phys. Rev. Lett.* **63**, 1996 (1989); S. Etemad, D. E. Aspnes, M. K. Kelley, R. Thompson, J. M. Tarascon, and G. W. Hull, *Phys. Rev. B* **37**, 3396 (1988).
- <sup>31</sup>S. L. Cooper, G. A. Thomas, J. Orenstein, D. H. Rapkine, A. J. Millis, S-W. Cheong, A. S. Cooper, and Z. Fisk, *Phys. Rev. B* **41**, 11605 (1990).
- <sup>32</sup>S. Tajima, S. Tanaka, T. Ido, and S. Uchida (unpublished).
- <sup>33</sup>C. N. Berglund and H. J. Braun, *Phys. Rev.* **164**, 790 (1967); C. Lee, J. Destry, and J. L. Brebner, *Phys. Rev. B* **11**, 2299 (1975).
- <sup>34</sup>A. S. Barker, Jr., H. W. Verleur, and H. J. Guggenheim, *Phys. Rev. Lett.* **17**, 1286 (1966).
- <sup>35</sup>I. Balberg and J. I. Pankove, *Phys. Rev. Lett.* **27**, 596 (1971).
- <sup>36</sup>A. S. Barker, Jr. and J. P. Remeika, *Phys. Rev. B* **10**, 987 (1974).